

Advances Toward Image Understanding of Multimodal Volume Data

Terry S. Yoo

National Library of Medicine,
The National Institutes of Health, 8600 Rockville Pike, Bethesda, MD 20894, USA

Abstract

This paper introduces new work in multiscale image statistics, a local framework that supports adaptive measurement of image structure where data may be represented by multiple incommensurable values. Data such as those represented by the Visible Human Project data often include multiple modalities such as color channels, multiple pulse sequences of magnetic resonance imaging, and X-ray CT data. Multiscale statistics can establish local correlations, covariances, and entropy measurements across the image. Such measurements have applications in nonlinear filtering, texture analysis, deformable registration and image segmentation.

1. Introduction and Background

When digital images are considered as arrays of observations made of an underlying scene, the vocabulary and calculus of statistics may be applied to their analysis. If an image is subject to noise in pixel measurement, it should be presented within the context of either known or computed properties of the pixel values. These properties include the sample size or raster resolution and other statistics such as the variance of the additive noise.

1.1. Statistical Analysis

Statistical pattern recognition is a discipline with a long and well-established history. Typically, statistical methods in image processing employ the distribution of intensities computed at the maximum outer scale of the image. That is, the histograms, mixture models, or probability distribution approximations are computed across the whole image, including all pixel values equally. Exceptions to this generalization include the contrast enhancement methods for adaptive histogram equalization (AHE). AHE and its derivatives construct local histograms of image intensity and compute new image values that generate an equalized local probability distribution. [7]. Related exceptions include median filtering, Markov random fields [4] and sigma filters [6]. These are related areas that are separate from the research presented in this paper.

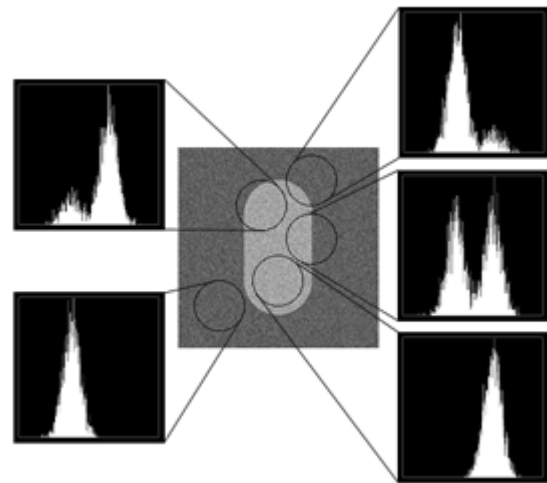


Figure 1. Test figure with local histograms. Histograms of pixel intensities shown for the local regions depicted by the gray circles. Note the changing symmetry of the local histograms depending on the overlap of the neighborhood, the figure, and the background.

1.2. Local Statistics of Image Intensity

As with most statistical pattern recognition systems, this research is based on the assumption that the input signal follows a Gibbs distribution. Stated loosely, this implies that the value for the intensity at a particular location has compact local support. In the context of local statistics of image patterns, a statistical measurement is expected to be consistent over a local neighborhood. Modest changes in the size and the location of the measurement region should induce smooth changes in the extracted statistics.

Consider the lozenge shaped object in Figure 1. The foreground pixel intensity has a mean brightness of 64 units, and the background has a mean of 0 units. The image has uncorrelated Gaussian distributed additive “white” noise, zero-mean with a standard deviation of 16 units. The image is 256×256 pixels. If distributions of local neighborhoods within the image are considered, more specific conclusions can be drawn, and conjectures can be made that accurately describe the geometry of the image. Figure 1 also shows five histograms of five local regions from the image. When the local region is taken

from only the foreground or only from the background intensities, a simple distribution with a single mode arises. When the local neighborhood is evenly balanced between object and background, a symmetric bimodal distribution is generated. Finally, when the number of foreground and background pixels is not evenly balanced, a skewed distribution results, with the skew favoring the pixel values that appear in greater number.

As the sample neighborhood smoothly varies its location, certain patterns arise. For example, a local region with a balanced bimodal distribution of intensities suggests a boundary between two regions. As the location of the local sampling region is perturbed, nearby locations where similar conditions of balanced bimodal intensity distributions are exposed. Following the set of all connected loci where this condition is met will extrude a perimeter where boundariness can be evaluated. More-over, the histograms themselves suggest a means of determining the strength of that boundary, even relative to the noise in the image. The separation between the two modes can be evaluated relative to the spread or dispersion of intensity values about the modes.

While the combined set of local histograms can be illuminating, it is unwieldy to generate and analyze a local histogram for each pixel in the image. A more compact description of the distribution of local image intensities is desired. One means of describing a probability distribution is through the generation of its central moments, a series of descriptive statistics. In the case of image analysis, *multiscale image statistics* not only capture the local intensity distribution, they can also be calculated directly from the image without the intermediate step of first generating local histograms.

2. Multiscale Statistics

Without *a priori* knowledge of the boundaries and the object widths within an image, locally adaptive multiscale statistical measurements are required to analyze the probability distribution across an arbitrary region of an image. This section presents multiscale image statistics, a technique developed through this research for estimating central moments of the probability distribution of intensities at arbitrary locations within an image across a continuously varying range of scales. Related work on the first order absolute moment has been presented previously by Demi [2]. This paper is a separate formal presentation of the general form of multiscale image statistics.

Consider a set of observed values, $\bar{I}(x) \subset \mathbb{R}^1$, where for purposes of discussion the location $x \in \mathbb{R}^1$, but can easily be generalized to \mathbb{R}^n . The values of $\bar{I}(x)$ may be sampled over a local neighborhood about a location x with a weighting, $\omega(x)$, and the convolution operation \otimes ,

where

$$\bar{I}(x) \otimes \omega(x) = \int_{-\infty}^{\infty} \omega(\tau) \bar{I}(x - \tau) d\tau = \int_{-\infty}^{\infty} \omega(x - \tau) \bar{I}(\tau) d\tau \quad (1)$$

To avoid a preference in orientation or location, the sampling function should be invariant with respect to spatial translation and spatial rotation. Babaud [1], Eberly [3], Koenderink [5], ter Haar Romeny [8], and others suggest that the optimal sampling function is the Gaussian $G(\sigma, x)$, where the parameter σ is the sampling aperture.

$$\omega(x) = G(\sigma, x) = \frac{1}{\sigma\sqrt{2\pi}} e^{-\frac{x^2}{2\sigma^2}} \quad (2)$$

Throughout this section, multiscale statistics will be graphically illustrated using a step edge with additive noise as an input function (see Figure 2).

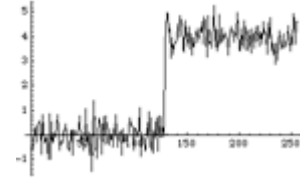


Figure 2. Example input signal $\bar{I}(x)$ - a noisy 1D step.

2.1. Multiscale Mean and Variance

Let the scale-space measurement comprised of a sum of the original image intensities weighted by a Gaussian sampling kernel be the average or expected value of $\bar{I}(x)$ over the neighborhood with an aperture of size σ . Thus:

$$\begin{aligned} \mu_{\bar{I}}(x | \sigma) &= \langle \bar{I}(x); \sigma \rangle = \int_{-\infty}^{\infty} G(\sigma, x - \tau) \bar{I}(\tau) d\tau \\ &= \bar{I}(x) \otimes G(\sigma, x) \end{aligned} \quad (3)$$

where $\langle \bar{I}(x); \sigma \rangle$ is read as mean or the expected value of $\bar{I}(x)$ measured with aperture σ . Figures 3a, 3e, and 3i, show the multiscale mean operator, applied to the test signal of Figure 2, at three different scales.

The multiscale variance is easily generalized from the definition of central moments. Equation (4) describes the local variance of intensity about a point x at scale σ .

$$\begin{aligned} \mu_{\bar{I}}^{(2)}(x | \sigma) &= \langle (\bar{I}(x) - \mu_{\bar{I}}(x | \sigma))^2; \sigma \rangle \\ &= \int_{-\infty}^{\infty} G(\sigma, x - \tau) (\bar{I}(\tau) - \mu_{\bar{I}}(x | \sigma))^2 d\tau \\ &= G(\sigma, x) \otimes (\bar{I}(x))^2 - (\mu_{\bar{I}}(x | \sigma))^2 \end{aligned} \quad (4)$$

Figures 3b, 3f, and 3j, show the multiscale variance operator applied at three different scales. Note that the maximum of the variance function localizes about the discontinuity and remains in the same location as scale

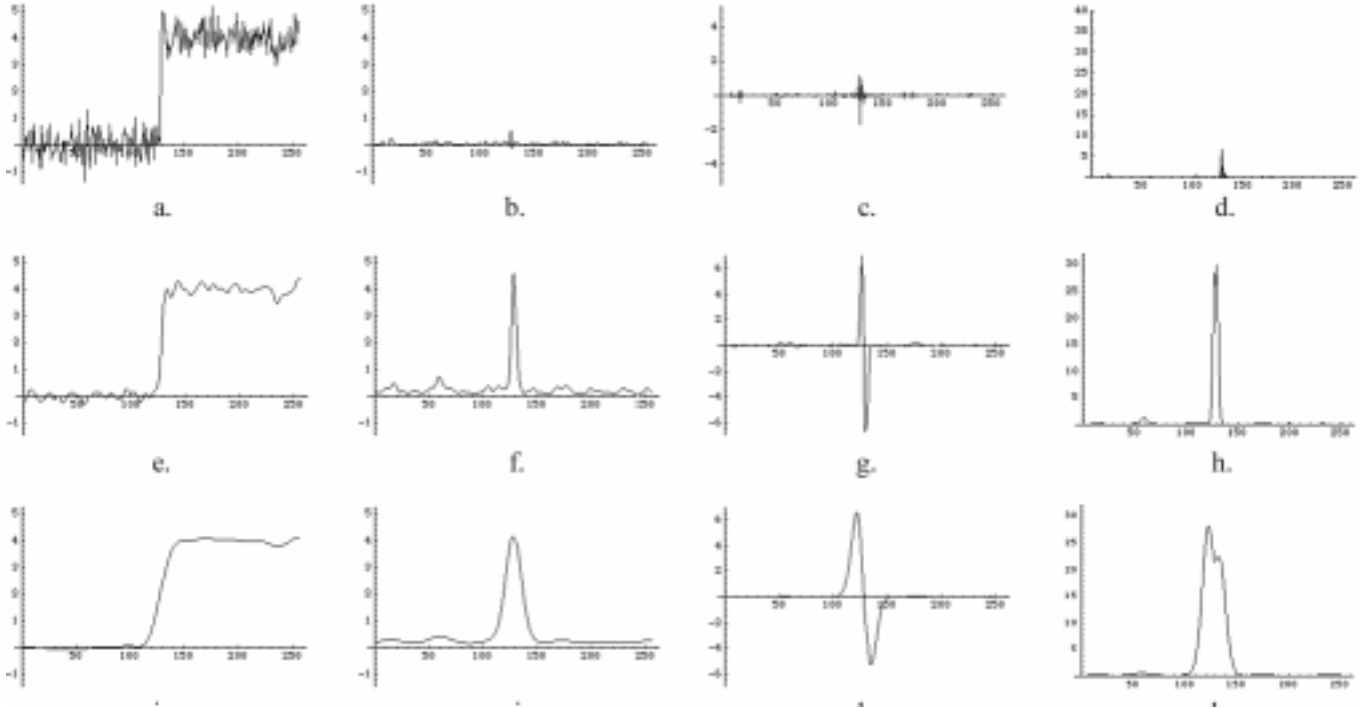


Figure 3. Multiscale statistics of the signal from Fig. 2, measured with apertures of different scales. The rows show $\sigma = 1$, $\sigma = 16$, and $\sigma = 32$, from top to bottom. The columns show the order k of the central moment with $k = 1$, $k = 2$, $k = 3$, $k = 4$, from left to right. Thus, the multiscale mean values are shown in Fig. 3a = $\mu_{\bar{I}}(x | 1)$, Fig. 3e = $\mu_{\bar{I}}(x | 16)$, and Fig. 3i = $\mu_{\bar{I}}(x | 32)$. Multiscale variances are shown in Fig. 3b = $\mu^{(2)}_{\bar{I}}(x | 1)$, Fig. 3f = $\mu^{(2)}_{\bar{I}}(x | 16)$, and Fig. 3j = $\mu^{(2)}_{\bar{I}}(x | 32)$. The remaining figures show the multiscale 3rd and 4th order central moments from left to right respectively.

changes. This behavior is similar to the gradient magnitude operator. Both are invariant with respect to rotation and translation, and both have similar responses to a given input stimulus.

2.2. Other Multiscale Central Moments

The general form for the multiscale central moment of order k of $\bar{I}(x)$ is given by

$$\begin{aligned} \mu_{\bar{I}}^{(k)}(x | \sigma) &= \left\langle \left(\bar{I}(x) - \mu_{\bar{I}}(x | \sigma) \right)^k ; \sigma \right\rangle \\ &= G(\sigma, x) \otimes \left(\bar{I}(x) - \mu_{\bar{I}}(x | \sigma) \right)^k \\ &= \int_{-\infty}^{\infty} G(\sigma, x - \tau) \left(\bar{I}(\tau) - \mu_{\bar{I}}(x | \sigma) \right)^k d\tau \end{aligned} \quad (5)$$

Figures 3c, 3g, and 3k show the multiscale responses of the 3rd order central moments of the function from Figure 2, and Figures 3d, 3h, and 3l, show the multiscale responses of the 4th order central moments. The 3rd order central moment (reflecting skew) has a zero crossing at the locus of the discontinuity that persists through changes in scale. Similarly, the 4th order moment has a local minimum at the discontinuity. This local minimum also persists through increasing scale.

3. Multiscale Statistics of 2D Images

Extending the construction of multiscale statistics to images of two and three dimensions is straightforward. The central moments are constrained to be invariant with respect to rotation as well as translation. These constraints specify an isotropic Gaussian as the sampling kernel. The general form for the k -th multiscale central moment for 2D images is

$$\begin{aligned} \mu_{\bar{I}}^{(k)}(\mathbf{p} | \sigma) &= \left\langle \left(\bar{I}(\mathbf{p}) - \mu_{\bar{I}}(\mathbf{p} | \sigma) \right)^k ; \sigma \right\rangle \\ &= G(\sigma, \mathbf{p}) \otimes \left(\bar{I}(\mathbf{p}) - \mu_{\bar{I}}(\mathbf{p} | \sigma) \right)^k \\ &= \frac{1}{\sigma^2 2\pi} \int_{-\infty}^{\infty} \int_{-\infty}^{\infty} e^{-\frac{((p_x - \tau)^2 + (p_y - \nu)^2)}{2\sigma^2}} \left(\bar{I}(\tau, \nu) - \mu_{\bar{I}}(\mathbf{p} | \sigma) \right)^k d\tau d\nu \end{aligned} \quad (6)$$

4. Multimodal Multiscale Image Statistics

The images of Fig. 4cde are three local statistical measurements made of the multimodal source images show in Fig. 4ab using an aperture whose spatial aperture is 2 pixels wide. Fig. 4c is the variance measure of Fig. 4a. Fig. 4e is the variance measure of Fig. 4b. Fig. 4d is the covariance of these two intensity values.

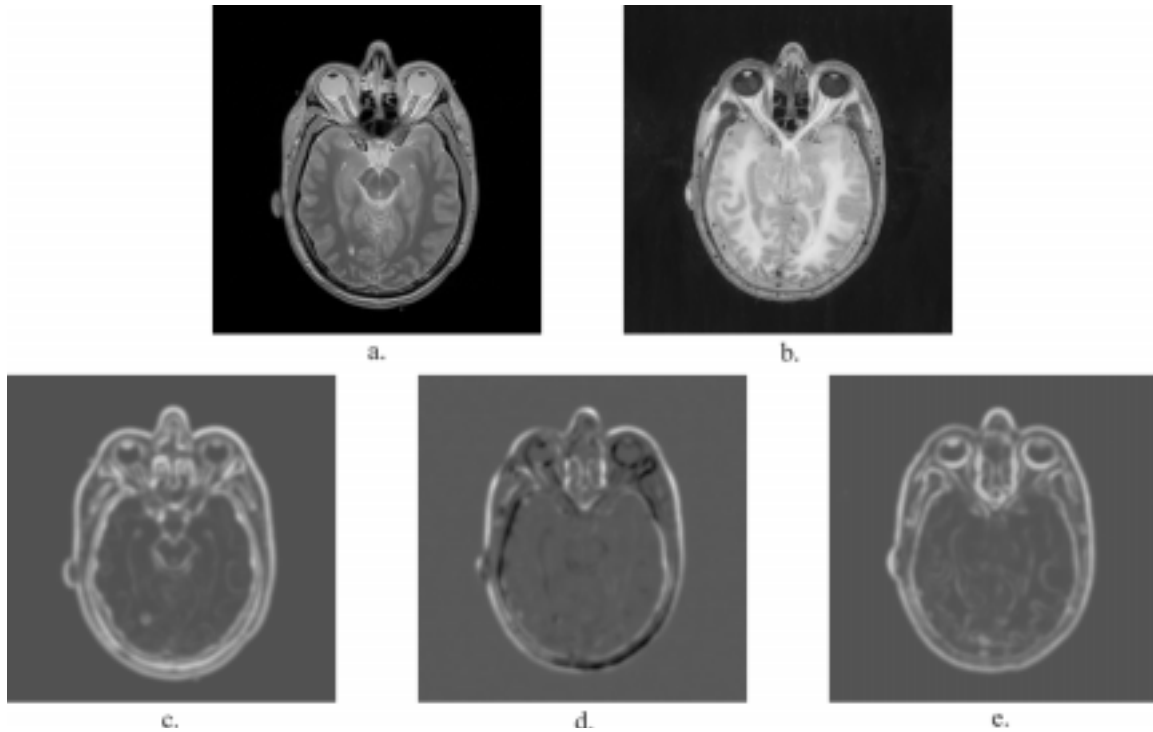


Figure 4. Multiscale statistics of a multimodal image from the Visible Human Project data. Figs. 4a and 4b are a PD weighted MRI image and the red channel of the corresponding cryosection data, respectively. Figs. 4c and 4e are variance measures of the respective source images. Fig. 4d is the local covariance measure of the two data slices. In all cases, $\sigma = 2$ pixel-widths.

Figure 4 demonstrates aspects of multimodal statistical representations that are significant with respect to image processing tasks. The variance image reflects edge strength and is analogous to the squared multiscale gradient magnitude of intensity. The covariance is some measure supporting mutual information, reflecting the fitness of the registration of the two image modalities.

5. Discussion and Future Work

Multiscale image statistics are a new means of capturing image geometry. Moreover, these measurements are invariant with respect to rotation, translation, and zoom, and they can be normalized to be invariant with respect to linear functions of intensity. They need to be extended to include entropy and other measures that may better support registration and segmentation tasks. Scaled statistics may support the analysis of images where vector valued methods are inappropriate (i.e., in the comparison of multimodal datasets) and in modalities such as MR where there are non-stationary properties to image noise. Multiscale image statistics are easily generalized to cover volume data. They are new and important tools in image processing of multimodal volume data.

References

- [1] Babaud, J., A. Witkin, and R.O. Duda. 1986. Uniqueness of the Gaussian kernel for scale-space filtering. *IEEE Trans. Patt. Anal. Mach. Intell.* PAMI-8: 2-14.
- [2] Demi, M. Contour Tracking by Enhancing Corners and Junctions. *Comp. Vision and Image Understanding*, 1996(63): 118-134.
- [3] Eberly, D. 1994. A differential geometric approach to anisotropic diffusion. in *Geometry-Driven Diffusion in Computer Vision*, ed. B.M. ter Haar Romeny, 371-392. Dordrecht, the Netherlands: Kluwer.
- [4] Geman S. and D. Geman. 1984. Stochastic relaxation, Gibbs distributions, and the Bayesian restoration of images. *IEEE Trans. Patt. Anal. Mach. Intell.* PAMI-6: 721-741.
- [5] Koenderink, J.J. 1984. The structure of images. *Biol. Cybernet* 50: 363-370.
- [6] Lee, J.S. 1983. Digital image smoothing and the sigma filter. *Comp. Vision, Graphics, and Image Processing*. CVGIP-24: 255-269.
- [7] Pizer, S.M., E.P. Amburn, J.D. Austin, R. Cromartie, A. Geselowitz, B.M. ter Haar Romeny, and J.B. Zimmerman. 1987. Adaptive histogram equalization and its variations. *Comp. Vision, Graphics, and Image Processing*. CVGIP-35: 355-368.
- [8] ter Haar Romeny, B.M. and L.M.J. Florack. 1991. A multiscale geometric approach to human vision. in *Perception of Visual Information*, ed. B. Hendee and P. N. T. Wells, 73-114. Berlin: Springer-Verlag.